DOI: 10.1002/ejic.200800290

Substituent Effects in the Solid-State Assembly of Silver(I) Complexes of 4-Substituted 3,6-Di(2-pyridyl)pyridazines

Edwin C. Constable,*[a] Catherine E. Housecroft,*[a] Markus Neuburger,[a] Sébastien Reymann,[a] and Silvia Schaffner[a]

Keywords: Heterocycle / Pyridazine / Pyridine / Silver / Coordination polymer

The reactions of one equivalent of silver(I) tetrafluoroborate with one equivalent of 4-R-3,6-di(2-pyridyl)pyridazine ligands (R = n-$C_{10}H_{21}$, 4-$O_2NC_6H_4$, 4-$MeOC_6H_4$, 4-$F_3CC_6H_4$, 4-NCC_6H_4, 3,5-$Br_2C_6H_3$, 3,5-$(MeO)_2C_6H_3$) in acetonitrile are reported. All complexes have been structurally characterized, and are found to belong to one of four different solid-state structure types: $[AgL_2][BF_4]$, $[Ag_2L_2][BF_4]_2$, $\{[Ag_3L_2][BF_4]_3\}_n$ and $\{[Ag_2(NCMe)_2L_2][BF_4]_2\}_n$. For the bulk samples of these compounds, elemental analyses are consistent with formulations of $[AgL_2][BF_4]$, $[Ag_2L_2][BF_4]_2$, but the two polymeric complexes analyse as 1:1 Ag:L complexes. In solution, ^1H and ^{13}C NMR spectra reveal only one ligand environment at room temperature for each product.

Introduction

The coordination chemistry of the 3,6-di(2-pyridyl)pyridazine (**1**) and related ligands is diverse.[1] In the free ligand, **1** contains a *trans*,*trans*-configuration (Scheme 1), but one can envisage that a switch to a *cis*,*cis*-configuration upon coordination permits **1** to function as a bis(bidentate) ligand, leading to the formation of a dinuclear complex with square-planar metal centres, or a tetranuclear grid when the metal centres are close to tetrahedral (Scheme 1). The latter self-assembly was first observed by Osborn and co-workers in the reaction of **1** with copper(I),[2] and more recently by Dunbar for silver(I).[3] The former has been observed with silver(I), but only when the ligand is substituted in the 4-position with a phenyl ring (ligand **2**, Scheme 2).[4] In contrast, the 1:1 reaction of **1** with AgO_3SCF_3 in $MeNO_2$ unexpectedly yields $[Ag(\mathbf{1})_2][O_3SCF_3]_2$ in which two nitrogen donor atoms remain non-coordinated. However, in solution, ^1H NMR spectrosopic data are consistent with species with a 1:1 stoichiometry.[4] Even more surprising is the observation that introducing a trimethylsilyl group into the 4-position of ligand **1** (ligand **3**, Scheme 2) results in the formation of the pentanuclear, silver-centred complex $[Ag_5(\mathbf{3})_4]^{5+}$ when equimolar amounts of $AgBF_4$ and **3** react in acetonitrile.[5] With a d^{10} configuration, silver(I) is a flexible coordination centre and can adopt coordination numbers of between two and eight.[6] Recently, Hanton has reviewed all complexes containing square-planar silver(I) centres and concludes that "predicting the precise requirements for the formation of a square planar Ag^I centre remains difficult".[6] Recently, we described the synthesis and characterization of a wide range of 4-substituted and 4,5-disubsti-

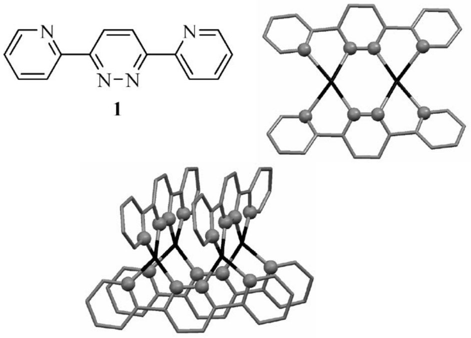

Scheme 1. Structure of ligand **1** and metal binding to give a dinuclear, near-planar motif or a tetranuclear grid.

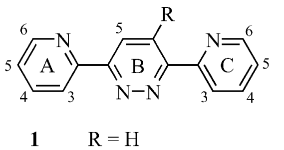

1 R = H
2 R = Ph
3 R = $SiMe_3$
4 R = n-$C_{10}H_{21}$
5 R = 4-NCC_6H_4
6 R = 4-$O_2NC_6H_4$
7 R = 4-$MeOC_6H_4$
8 R = 4-$F_3CC_6H_4$
9 R = 3,5-$Br_2C_6H_3$
10 R = 3,5-$(MeO)_2C_6H_3$

Scheme 2. Structures of ligands **1** to **10** with ring labelling used for NMR spectroscopic assignments; the aryl substituent is ring D.

---

[a] Department of Chemistry, University of Basel,
Spitalstrasse 51, 4056 Basel, Switzerland
Fax: +41-61-267-1018
E-mail: catherine.housecroft@unibas.ch

tuted 3,6-di(2-pyridyl)pyridazines as a prelude to an investigation of their complex formation.[7] We now report a study of the reactions of silver(I) tetrafluoroborate with seven 4-substituted 3,6-di(2-pyridyl)pyridazines (**4**–**10**, Scheme 2) and the solid-state structures of the isolated complexes.

Results and Discussion

To ensure that the study of the complexation reactions of silver(I) with pyridazines **4** to **10** was comparative, all reactions were carried out using equimolar amounts of silver(I) tetrafluoroborate and the ligand under the same conditions (in MeCN, 5 min sonication at room temperature followed by 15 min heating at reflux) with concentrations in the range 1.5×10^{-6} to 3.6×10^{-6} mol dm^{-3}. The products were precipitated by adding a large excess of diethyl ether to CH_2Cl_2 or MeCN solutions of the crude products. ^1H and ^{13}C NMR spectra of CD_3CN solutions of the purified complexes showed the presence of one ligand environment for each complex. Elemental analytical data were consistent with the formation of complexes of empirical formulae $[AgL_2][BF_4]$ (L = **4** and **10**) and $[AgL][BF_4]$ (L = **5**, **6**, **7**, **8** and **9**). FAB mass spectrometric data for bulk samples of each silver(I) complex with the pyridazines **4** to **10** showed the same fragmentation pattern. The highest mass peak in each case was assigned to $[Ag_2L_2BF_4]^+$ followed by lower mass peak envelopes consistent with $[AgL_2]^+$ and $[AgL]^+$ (see experimental section for data).

We have previously shown[8,9] that crystalline samples of either $[Ag_2L_2][CF_3SO_3]_2$ or $[Ag_2L_3][CF_3SO_3]_2$ can be isolated from reactions of 3,6-di(2-pyridyl)-1,2,4,5-tetrazine with $[AgCF_3SO_3]$, while solution data suggest the presence of 1:1 complexes with excess ligand being involved in exchange with coordinated ligand to give, on average, only one ligand environment on the NMR timescale at room temperature. Thus, even with a common counterion, structural variation is achievable in the solid state and, therefore, it is difficult to draw meaningful conclusions about coordination patterns from the solution spectroscopic data presented for the reactions of $AgBF_4$ with ligand **4** to **10**. X-ray quality crystals of each product were obtained, and crystallographic investigations revealed surprisingly diverse coordination modes for the ligands.

Yellow plates of $[Ag(\mathbf{4})_2][BF_4]$ were grown by slow diffusion of Et_2O into an MeCN solution of the complex. The solid-state structure of $[Ag(\mathbf{4})_2][BF_4]$ contains two crystallographically independent, but similar, $[Ag(\mathbf{4})_2]^+$ cations. Figure 1 shows the molecular structure of one cation, and the caption gives selected bond parameters for both. The 1:2 stoichiometry was consistent with the elemental analysis of the bulk sample. The coordination environment of the silver(I) ion is pseudo-square planar, being constrained by the ligand bite angles of about 70°, and with a deviation of Ag1 from the least-squares plane through the four N atoms of 0.064 Å. Bond lengths and angles within the aromatic rings of the ligands are as expected.[7,10–15] Free 3,6-di(2-pyridyl)-pyridazine ligands adopt a *trans,trans* arrangement.[7,10–15] In $[Ag(\mathbf{4})_2][BF_4]$, coordination of ligand **4** to one silver(I) ion leads to a conformational change to a *cis,trans* arrangement. Of the two non-coordinated nitrogen atoms in the Ag1-containing cation, N4 is involved in an interaction with the silver(I) centre of an adjacent cation [Figure 2, Ag···N4^a 2.98(1) Å; symmetry code a = –*x*, 1 – *y*, 1 – *z*]. The stacking interaction is extended by a close Ag1···Ag1^c contact of 3.438(1) Å; symmetry code a = 1 – *x*, 1 – *y*, 1 – *z*. Figure 2 illustrates the offset N4···Ag1···Ag1···N4 stacks that result. In contrast, the Ag2-containing cations form pairs with Ag···Ag separations of 3.538(2) Å, with pairs of cations assembling through π-stacking of heterocyclic rings. The decyl chains are in an extended conformation and are packed with van der Waals forces between adjacent chains.

Ligand **10** also forms a 1:2 complex with silver(I) and X-ray quality yellow prisms of $[Ag(\mathbf{10})_2][BF_4]$ were grown by slow diffusion of Et_2O into a MeCN solution of the complex. Figure 3 shows the molecular structure of the cation, and illustrates the *cis,trans*-conformation of the coordinated ligand. Atom Ag1 lies on an inversion centre and the AgN_4 unit is strictly planar. Whereas the angles between the least-squares planes of the coordinated heterocyclic rings in $[Ag(\mathbf{4})_2]^+$ are 19.2(5) and 15.1(4)°, and 9.6(5) and 12.7(5)°

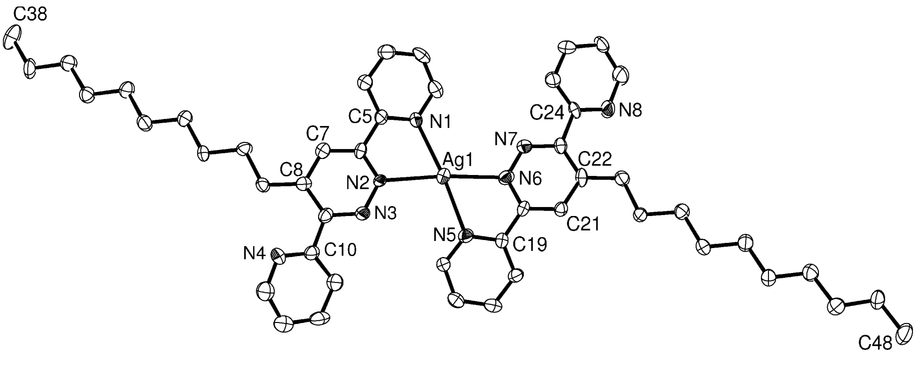

Figure 1. Molecular structure of one of the independent cations (labelled cation A) in $[Ag(\mathbf{4})_2][BF_4]$; ellipsoids are plotted at the 40% probability level, and H atoms are omitted. Selected bond parameters for cation A: Ag1–N1 2.336(6), Ag1–N2 2.381(6), Ag1–N5 2.361(6), Ag1–N6 2.357(7) Å; N1–Ag1–N2 69.8(2), N1–Ag1–N6 116.1(2), N5–Ag1–N6 69.4(2), N2–Ag1–N5 104.5(2)°, and for cation B: Ag2–N51 2.266(6), Ag2–N52 2.421(7), Ag2–N55 2.305(6), Ag2–N56 2.497(7) Å; N51–Ag2–N52 69.4(2), N51–Ag2–N56 114.5(3), N55–Ag2–N56 69.7(2), N52–Ag2–N55 106.4(2)°.

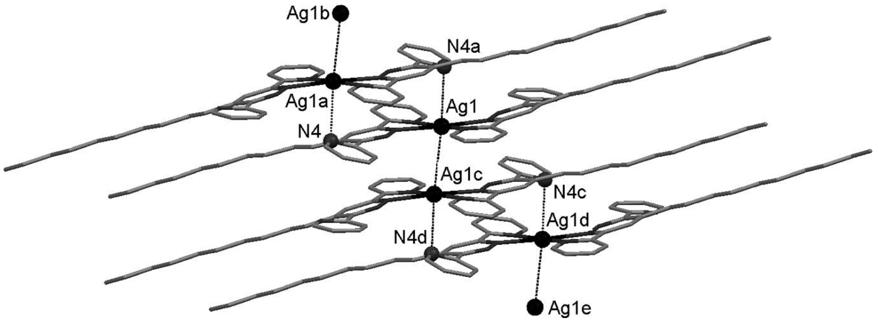

Figure 2. Assembly of stacks of the Ag1-containing cations in $[Ag(\mathbf{4})_2][BF_4]$, symmetry codes: a = –*x*, 1 – *y*, 1 – *z*; b = –1 + *x*, *y*, *z*; c = 1 – *x*, 1 – *y*, 1 – *z*; d = 1 + *x*, *y*, *z*; e = 2 – *x*, 1 – *y*, 1 – *z*.

for the two independent cations, those in $[Ag(\mathbf{10})_2]^+$ are significantly larger [33.0(1)°]. In contrast to the packing in $[Ag(\mathbf{4})_2][BF_4]$ where Ag···Ag and $Ag\cdots N_{py}$ close contacts are dominant, cations in $[Ag(\mathbf{10})_2][BF_4]$ assemble so that each silver atom is sandwiched between two pyridine rings as shown in Figure 4, although the rings are slipped with respect to one another giving two η^2-modes of interaction. The closest contacts are $Ag1\cdots C10^b$ 3.310(3) Å and $Ag1\cdots C11^b$ 3.254(3) Å (symmetry code b = *x*, –1 + *y*, *z*), and the $Ag\cdots py_{centroid}$ distance of 3.34 Å is at the longer end of the range quoted for η^6 interactions.[16] Much shorter contacts have been observed in organosilver(I) systems.[17] The offset stack of cations shown in Figure 4 is connected to an adjacent stack by hydrogen bonds involving methoxy atom O1 and a CH group in a pyridine ring containing atom N4 [$O1\cdots H131^cC13^c$ 2.38 Å, $O1\cdots C13^c$ 3.319(4) Å, $O1\cdots H131^c–C13^c$ 166°; symmetry code c = $^3/_2$ – *x*, $^3/_2$ + *y*, $^3/_2$ – *z*].

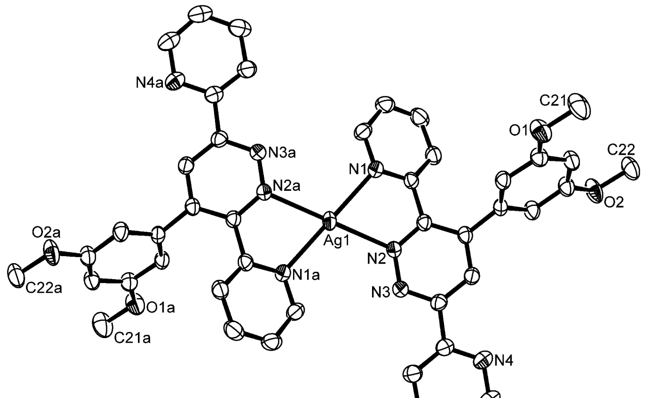

Figure 3. Molecular structure of the $[Ag(\mathbf{10})_2]^+$ cation in $[Ag(\mathbf{10})_2]$-$[BF_4]$; ellipsoids are plotted at the 40% probability level. H atoms and anions are omitted. Symmetry code a = –*x* + $^1/_2$, –*y* + $^1/_2$, –*z*. Selected bond parameters: Ag1–N1 2.304(2), Ag1–N2 2.374(2) Å, N1–Ag1–N2 71.23(7), N1–Ag1–$N2^a$ 108.77(7)°.

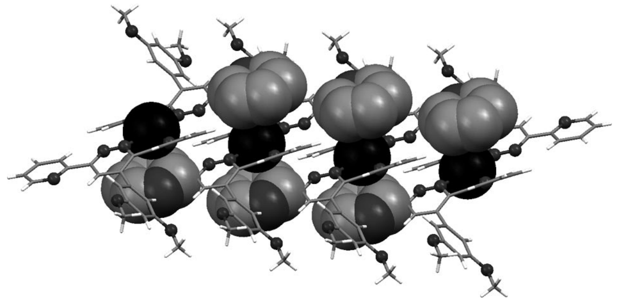

Figure 4. Packing of $[Ag(\mathbf{10})_2]^+$ cations in $[Ag(\mathbf{10})_2][BF_4]$. The pyridine–Ag–pyridine sandwiches are shown in space-filling representations; other N and O atoms are shown in ball-and-stick representations.

Crystalline products of the 1:1 reactions of ligands **5**, **8** and **9** with silver(I) tetrafluoroborate proved to be 2:2 complexes. X-ray quality crystals were grown in each case by diffusion of Et_2O vapour into MeCN solutions of the crude product. The $[Ag_2(\mathbf{5})_2]^{2+}$ cation in $[Ag_2(\mathbf{5})_2][BF_4]_2$ is shown in Figure 5, and the structural motif is similar to that observed for $[Ag_2L_2]^{2+}$ in $[Ag_2L_2][CF_3SO_3]_2$ where L = 3,6-di(2-pyridyl)-1,2,4,5-tetrazine.[8,18] The two silver centres in $[Ag_2(\mathbf{5})_2]^{2+}$ are related by a centre of symmetry, and the coordination sphere is distorted planar, with two short [2.213(2) and 2.237(2) Å] and two long [2.505(2) and 2.738(2) Å] Ag–N bonds. Figure 5 illustrates that the pyridazine ring is significantly twisted with respect to the two pyridine rings of the ligand [angles between the least-squares planes of the rings containing N1 and N2/N3, and N4 and N2/N3 are 44.1(1) and 24.5(1)°]. The cations are aligned in offset stacks so that N4-containing pyridine rings are π-stacked (distances between rings: 3.37 Å, Figure 6). This interaction is complemented by an η^2-interaction involving two C atoms in the N4-containing pyridine ring on one side of the silver centre [$Ag1\cdots C12^b$ 3.412(3), $Ag1\cdots C13^b$ 3.414(3) Å; symmetry code b = *x*, 1 + *y*, *z*]. The Ag atom deviates significantly (0.166 Å) from the least planes plane containing the four N donor atoms, being displaced towards the η^2 interaction. On the opposite side of the AgN_4 plane, atom Ag1 engages in a contact with the $[BF_4]^-$ ion [$Ag1\cdots F4$ 3.885(3) Å]. The rows of cations are interlinked by non-classical hydrogen bonding between the cyano N atom and a pyridine CH unit [$N5\cdots H21^cC2^c$ 2.50 Å, $N5\cdots C2^c$ 3.201(4) Å, $N5\cdots H21^c–C2^c$ 131°; symmetry code *x*, $^1/_2$ – *y*, $^1/_2$ + *z*].

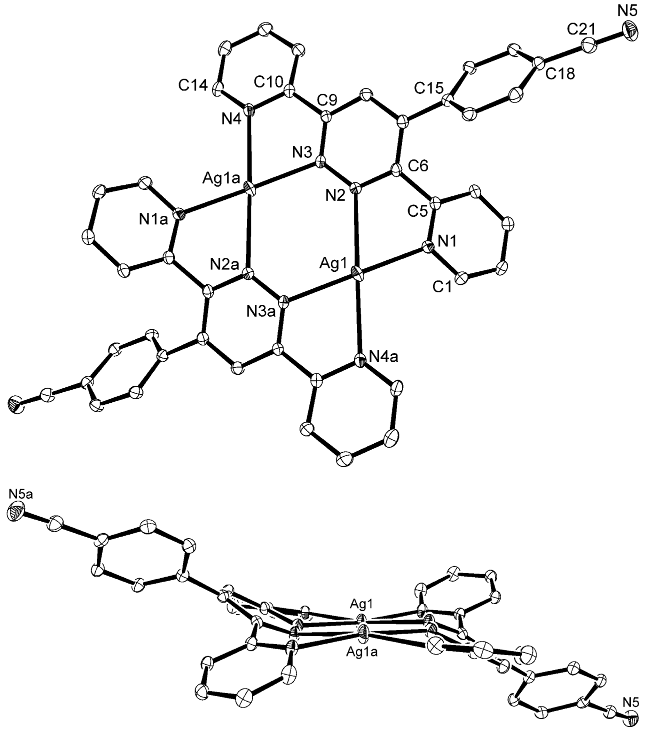

Figure 5. Molecular structure of the $[Ag_2(\mathbf{5})_2]^{2+}$ cation in $[Ag_2(\mathbf{5})_2]$-$[BF_4]_2$; ellipsoids are plotted at the 40% probability level, and H atoms are omitted. Selected bond lengths are angles: Ag1–N1 2.213(2), Ag1–N2 2.738(2), Ag1–N3^a 2.237(2), Ag1–N4^a 2.505(2), C7–C15 1.486(3), C18–C21 1.436(4), N5–C21 1.141(4), Ag1···Ag1^a 4.206 Å; N4^a–Ag1–N3^a 70.45(8), N4^a–Ag1–N1 111.24(8), N3^a–Ag1–N2 109.81(8), N1–Ag1–N2 67.35(7)° (symmetry code a = –*x*, –*y*, –*z*). The lower diagram shows the bending of the pyridazine rings away from the coordination plane.

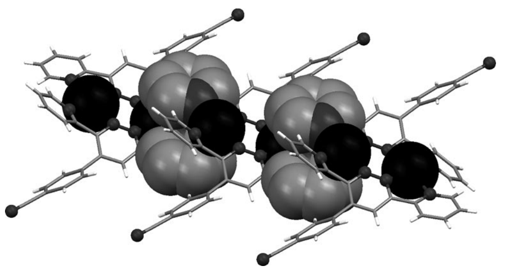

Figure 6. Packing of $[Ag_2(\mathbf{5})_2]^{2+}$ cations in $[Ag_2(\mathbf{5})_2][BF_4]_2$. The Ag atoms and N4-containing pyridine rings involved in η^2-contacts are shown in space filling representations; other N atoms are shown in ball-and-stick representations.

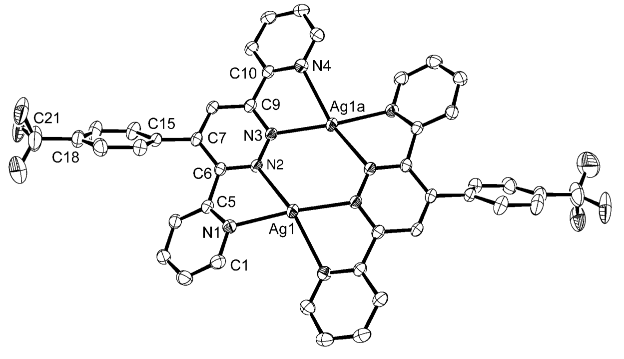

Figure 7. Molecular structure of the $[Ag_2(\mathbf{8})_2]^{2+}$ cation in $[Ag_2(\mathbf{8})_2]$-$[BF_4]_2$·2.6MeCN; ellipsoids are plotted at the 40% probability level. H Atoms and anions are omitted. Only one set of F atoms of each disordered CF_3 group is shown. Selected bond parameters: Ag1–N1 2.311(2), Ag1–N2 2.384(2), Ag1–N4^a 2.477(2), Ag1–N3^a 2.273(2), Ag1···Ag1^a 3.6437(3) Å; N1–Ag1–N2 71.11(6), N1–Ag1–N4^a 102.56(6), N3^a–Ag1–N2 120.43(6), N4^a–Ag1–N3^a 70.64(6)°. Symmetry code: a = –*x*, –*y*, –*z*.

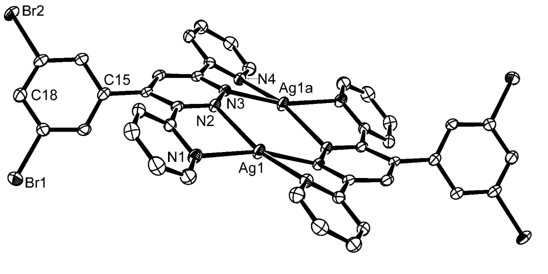

Figure 8. Molecular structure of the $[Ag_2(\mathbf{9})_2]^{2+}$ cation in $[Ag_2(\mathbf{9})_2]$-$[BF_4]_2$·2MeCN; ellipsoids are plotted at the 40% probability level. H Atoms and anions are omitted. Selected bond parameters: Ag1–N1 2.355(4), Ag1–N2 2.369(3), Ag1–N4^a 2.430(3), Ag1–N3^a 2.312(3), Ag1···Ag1^a 3.691(1) Å; N1–Ag1–N2 70.4(1), N1–Ag1–N4^a 103.6(1), N3^a–Ag1–N2 119.9(1), N4^a–Ag1–N3^a 70.6(1)°. Symmetry code: a = –*x*, –*y*, –*z*.

Crystalline $[Ag_2(\mathbf{8})_2][BF_4]_2$ and $[Ag_2(\mathbf{9})_2][BF_4]_2$ were isolated as the acetonitrile solvates $[Ag_2(\mathbf{8})_2][BF_4]_2$·2.6MeCN and $[Ag_2(\mathbf{9})_2][BF_4]_2$·2MeCN. Figures 7 and 8 show the structures of the $[Ag_2(\mathbf{8})_2]^{2+}$ and $[Ag_2(\mathbf{9})_2]^{2+}$ cations, each of which is centrosymmetric. The deviations of the coordinated ligands from planarity are similar to those observed in $[Ag_2(\mathbf{5})_2]^{2+}$; in $[Ag_2(\mathbf{8})_2]^{2+}$, the angles between the least-squares planes containing atoms N1 and N2/N3, and N4 and N2/N3 are 35.3(1) and 31.5(1)°, and the corresponding angles in $[Ag_2(\mathbf{9})_2]^{2+}$ are 34.9(2) and 28.9(2)°, respectively. In each of $[Ag_2(\mathbf{5})_2]^{2+}$, $[Ag_2(\mathbf{8})_2]^{2+}$ and $[Ag_2(\mathbf{9})_2]^{2+}$, the plane of the aryl substituent is twisted significantly out of the plane of the pyridazine ring {angles between least-squares planes are 52.5(1), 59.3(1) and 53.3(2)°, respectively, for $[Ag_2(\mathbf{5})_2]^{2+}$, $[Ag_2(\mathbf{8})_2]^{2+}$ and $[Ag_2(\mathbf{9})_2]^{2+}$}. The coordination environment about the silver centre in $[Ag_2(\mathbf{8})_2]^{2+}$ is distorted from planarity, the angles N1–Ag1–N3^a and N2–Ag1–N4^a (symmetry code a = –*x*, –*y*, –*z*) being 165.32(6) and 155.68(6)°, respectively. A similar distortion occurs in $[Ag_2(\mathbf{9})_2]^{2+}$, with the corresponding angles being 165.4(1) and 158.2(1)°. In $[Ag_2(\mathbf{8})_2]^{2+}$, the CF_3 groups are disordered and the F atom positions have been modelled over two sets with estimated site occupancy factors of 0.5.

The packing in $[Ag_2(\mathbf{8})_2][BF_4]_2$·2.6MeCN is dominated by cation···anion interactions, and, in contrast to the packing in $[Ag(\mathbf{4})_2]^+$, $[Ag(\mathbf{10})_2]^+$ and $[Ag_2(\mathbf{5})_2]^{2+}$, exhibits no close intercation Ag···Ag contacts and only one short Ag···C_{py} contact [Ag1···C14^i 3.386(2) Å; symmetry code i = $^1/_2 + x$, $^1/_2 + y$, *z*]. Figure 9 illustrates that Ag···F(anion) and CH(aryl)···F(anion) are the dominant packing interactions. The packing in $[Ag_2(\mathbf{9})_2][BF_4]_2$·2MeCN shares some features in common with $[Ag_2(\mathbf{8})_2][BF_4]_2$·2.6MeCN: no close

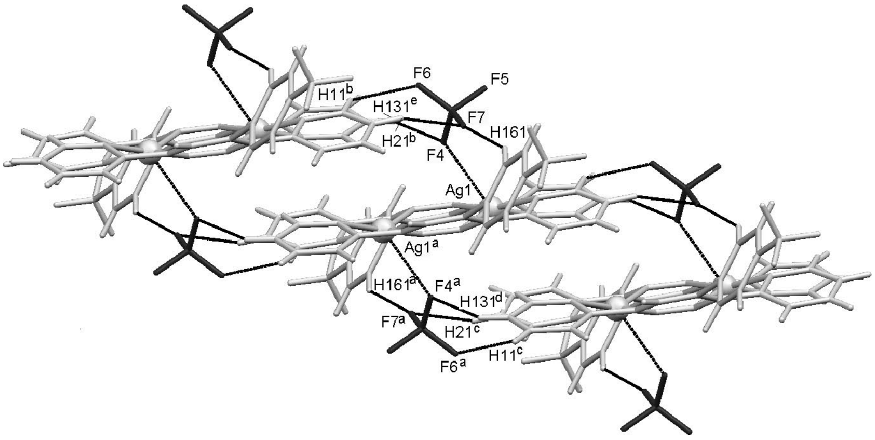

Figure 9. Packing of cations (pale grey) and anions (black) in $[Ag_2(\mathbf{8})_2][BF_4]_2$·2.6MeCN. Short contacts: Ag1···F4 2.808(2) Å; F7···H161–C16 2.54 Å, F7···C16 3.378(3) Å, F7···H161–C16 146°; F7···$H21^b$–$C2^b$ 2.45 Å, F7···$C2^b$ 3.338(3) Å, F7···$H21^b$–$C2^b$ 154°; F6···$H11^b$–$C1^b$ 2.49 Å, F6···$C1^b$ 3.177(3) Å, F6···$H11^b$–$C1^b$ 129°; F4···$H131^e$–$C13^e$ 2.51 Å, F4···$C13^e$ 3.232(3) Å, F4···$H131^e$–$C13^e$ 132°. Additional interaction not shown in the Figure: F5···$H121^f$–$C12^f$ 2.42 Å, F5···$C12^f$ 3.166(3) Å, F5···$H121^f$–$C12^f$ 134°. Symmetry codes: b = $^1/_2 + x$, $^1/_2 + y$, z; e = $-^1/_2 - x$, $-^1/_2 - y$, $-z$; f = $-x$, $-1 - y$, $-z$.

intercation Ag···Ag contacts, only one short Ag···C_{py} contact [Ag1···$C14^i$ 3.291(4) Å; symmetry code i = $-1 + x$, y, z], and extensive Ag···F(anion) and CH(aryl)···F(anion) interactions.

The ^1H and ^{13}C NMR spectra were consistent with a single ligand environment. Slow diffusion of Et_2O vapour into an MeCN solution of the bulk product unexpectedly gave rise to X-ray quality colourless plates of the polymer $\{[Ag_3(\mathbf{7})_2](BF_4)_3\}_n$. The complex crystallizes in the non-chiral $C2/c$ space group. The asymmetric unit and its assembly into a polymeric chain are illustrated in Figure 10. Atom Ag2 is three-coordinate with respect to nitrogen donors, and is related to $Ag2^a$ by an inversion centre which lies at the centre of a near planar Ag_2N_4 macrocycle which incorporates the N-donors of two pyridazine rings. One $[BF_4]^-$ ion coordinates on one side of the AgN_3 unit [Ag2···F3 2.720(3) Å]. Atom Ag1 is in a linear environment (see Figure caption), being coordinated to two pyridine N-donors, and a C_2 axis (parallel to the b axis) runs through each Ag1 atom. Each polymer chain runs parallel to the c-axis, and since the repeating unit of the chain contains a centre of symmetry, the polymer is achiral and are related to one another simply by translation (Figure 11). The principle building block in the $\{[Ag_3(\mathbf{7})_2]^{3+}\}_n$ chains can be viewed as being an $[Ag_2(\mathbf{7})_2]^{2+}$ unit similar to those observed in $[Ag_2(\mathbf{5})_2]^{2+}$, $[Ag_2(\mathbf{8})_2]^{2+}$ and $[Ag_2(\mathbf{9})_2]^{2+}$. However, whereas the angles between the least-squares planes of the pyridine and pyridazine rings in the latter are similar, those between the rings containing atoms N1 and N2/N4, and N3 and N2/N4 in each $[Ag_2(\mathbf{7})_2]^{2+}$ unit are significantly different [19.5(2) and 69.5(2)°]. The twisting of one pyridine ring switches the coordination environment of the silver(I) atom from four- to three-coordinate and at the same time, allows the pendant pyridine nitrogen donor to bind to another metal ion. This results in the propagation of a polymer chain with a 3:2 silver:ligand stoichiometry.

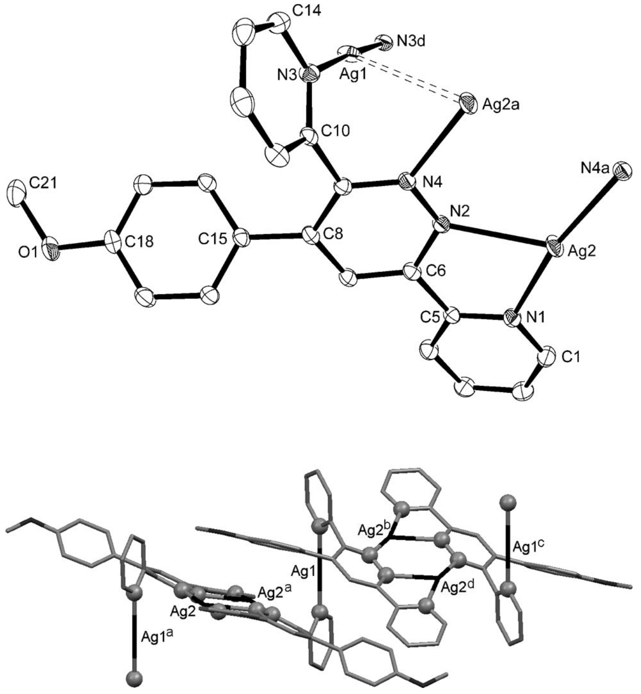

Figure 10. Top: Molecular structure of the asymmetric unit and coordination environments of Ag1 and Ag2 in $\{[Ag_3(\mathbf{7})_2][BF_4]_3\}_n$; ellipsoids are plotted at the 40% probability level. H atoms and anions are omitted. Selected bond parameters: Ag1–N3 = Ag1–$N3^d$ 2.138(2), Ag2–N1 2.214(2), Ag2–N2 2.416(2), Ag2···$Ag2^a$ 3.603 Å; N3–Ag1–$N3^d$ 176.4(1), N1–Ag2–N2 71.72(8), N1–Ag2–$N4^a$ 164.91(8), N2–Ag2–$N4^a$ 119.71(7)°. Bottom: part of one polymeric chain; Ag2–$N4^a$ 2.173(2), Ag1···$Ag2^a$ = Ag1···$Ag2^b$ 3.5517(2) Å. Symmetry codes: a = $-x$, $-y$, $-z$; b = x, $-y$, $^1/_2 + z$; c = $-x$, $-y$, $2 - z$, d = $-x$, y, $^3/_2 - z$.

The 1:1 reaction of $AgBF_4$ and ligand **6** gave a product, the FAB mass spectrum of which exhibited peaks assigned to $[Ag(\mathbf{6})]^+$ (m/z 462), $[Ag(\mathbf{6})_2]^+$ (m/z 817), and $[Ag_2(\mathbf{6})_2$-

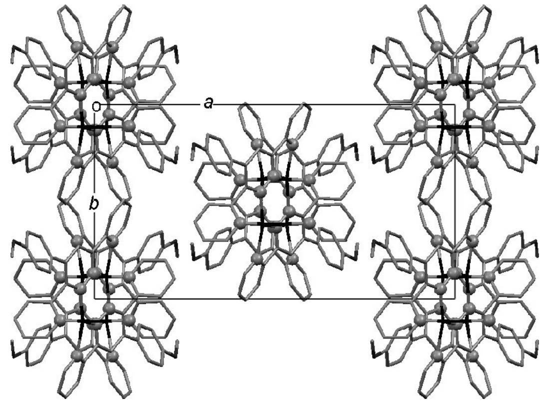

Figure 11. Packing of chains in $\{[Ag_3(\mathbf{7})_2][BF_4]_3\}_n$; H atoms and anions are omitted. Each chain runs parallel to the *c* axis. Ag atoms are shown in black, and N atoms are shown in ball representation.

$BF_4]^+$ (*m*/*z* 1013). The ^1H and ^{13}C NMR spectra showed only one ligand environment. However, X-ray quality yellow needles, grown by slow diffusion of Et_2O vapour into an MeCN solution of the product, proved to be of the polymer $\{[Ag_2(\mathbf{6})_2(NCMe)_2][BF_4]_2{\cdot}Et_2O\}_n$. The structure of one repeat unit of a polymer chain is depicted in Figure 12; for clarity, only the *ipso*-C atom of each $C_6H_4NO_2$ group is shown. There are two different silver(I) environments. Each silver atom is coordinated to two bpy domains, one from each of two different ligands with Ag–N bond lengths than lie in the range 2.274(7) to 2.766(7) Å; the fifth coordination site of each silver centre is occupied by an acetonitrile ligand. Both coordination spheres are irregular, as illustrated for Ag2 in Figure 9 (b). The polymer chain at the top of Figure 9 (a) is propagated by coordination of atoms N3 and N4 to $Ag2^b$ (symmetry code $b = 1 - x, -{}^1/_2 + y, {}^1/_2 - z$). The polymer chains are helical, but the complex crystallizes in the non-chiral space group $P2_1/c$, giving rise to a racemate as illustrated in Figure 11. Face-to-face π-interactions support the helical assembly and involve pairs of offset pyridine and aryl rings containing atoms N1 and C35, and N5 and C15, respectively. These interactions are weak, with interplane separations of between 3.65 and 3.86 Å. In addition, the π-system of the MeCN ligand containing atoms N11 and C41 is positioned close to the π-cloud of the pyridine ring containing N4 [closest contacts are $C12{\cdots}C41^c$ 3.40(2) Å, $C12{\cdots}N11^c$ 3.43(2) Å, symmetry code $c = 1 - x, -{}^1/_2 + y, {}^1/_2 - z$] (Figure 13).

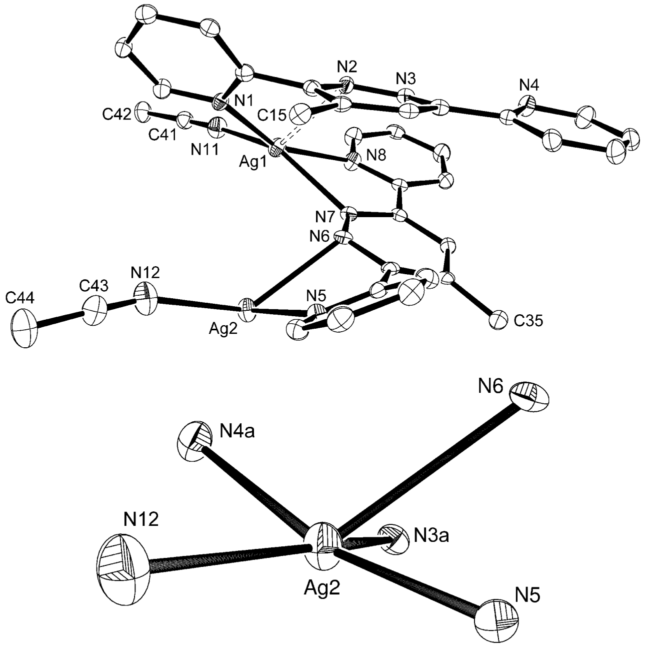

Figure 12. Top: Molecular structure of the asymmetric unit in $\{[Ag_2(\mathbf{6})_2(NCMe)_2][BF_4]_2{\cdot}Et_2O\}_n$ with H atoms, anions and Et_2O solvent molecules omitted; ellipsoids are plotted at the 20% probability level. Only the *ipso*-C atoms of the $C_6H_4NO_2$ substituents are shown. Selected bond parameters around Ag1: Ag1–N1 2.282(7), Ag1–N2 2.766(7), Ag1–N7 2.435(7), Ag1–N8 2.329(7), Ag1–N11 2.381(8) Å; N1–Ag1–N2 66.6(2), N1–Ag1–N7 109.9(2), N2–Ag1–N7 70.0(2), N2–Ag1–N8 91.5(2), N7–Ag1–N8 67.7(2), N1–Ag1–N11 95.9(3), N8–Ag1–N11 95.1(3)°. Bottom: coordination environment about Ag2 in the polymer chain: Ag2–N5 2.274(7), Ag2–N6 2.608(7), Ag2–N12 2.514(9) Å, $Ag2–N3^a$ 2.528(7), $Ag2–N4^a$ 2.303(7) Å; $N3^a–Ag2–N4^a$ 67.7(2), $N3^a–Ag2–N5$ 113.1(2), $N3^a–Ag2–N6$ 71.7(2), $N4^a–Ag2–N6$ 100.7(3), N5–Ag2–N6 68.2(2), $N4^a–Ag2–N12$ 91.0(3), N5–Ag2–N12 91.4(3), N6–Ag2–N12 130.5(3)°. (symmetry code $a = -x, {}^1/_2 + y, {}^1/_2 - z$).

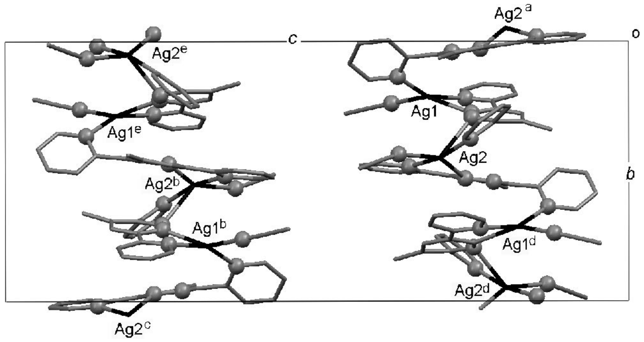

Figure 13. Helical chains of opposite chirality in the unit cell of $\{[Ag_2(\mathbf{6})_2(NCMe)_2][BF_4]_2{\cdot}Et_2O\}_n$. Only the *ipso*-C atoms of the $C_6H_4NO_2$ substituents are shown. Ag atoms are shown in black, and N atoms are shown in ball representation. Symmetry codes: $a = -x, {}^1/_2 + y, {}^1/_2 - z$; $b = -x, -y, -z$; $c = x, {}^3/_2 - y, {}^1/_2 + z$; $d = -x, {}^1/_2 + y, {}^1/_2 - z$; $e = x, {}^1/_2 - y, {}^1/_2 + z$.

Conclusions

The reactions of one equivalent of silver(I) tetrafluoroborate with one equivalent of 4-R-3,6-di(2-pyridyl)pyridazine ligands [R = n-$C_{10}H_{21}$, 4-$O_2NC_6H_4$, 4-$MeOC_6H_4$, 4-$F_3CC_6H_4$, 4-NCC_6H_4, 3,5-$Br_2C_6H_3$, 3,5-$(MeO)_2C_6H_3$] in acetonitrile are reported. All complexes have been structurally characterized, and are found to belong to one of four different solid-state structure types: $[AgL_2][BF_4]$, $[Ag_2L_2][BF_4]_2$, $\{[Ag_3L_2][BF_4]_3\}_n$ and $\{[Ag_2(NCMe)_2L_2][BF_4]_2\}_n$. For the bulk samples, elemental analyses are consistent with formulations of $[AgL_2][BF_4]$, $[Ag_2L_2][BF_4]_2$, but the two polymeric complexes analyse as 1:1 Ag:L complexes. It is difficult to rationalize the preference for one structure type over another in the solid state, but in solution, ^1H and ^{13}C NMR spectra reveal only one ligand environment at room temperature for each product. Attempts were made to see the single crystal structures corresponded to the structures of the bulk samples by using powder diffraction experiments. For the complexes containing ligands **4** and **8**, we were able to confirm that each bulk sample consisted of one single phase. In the case of the other samples the crystalline material appeared to have decayed (e.g. by solvent loss) and no useful conclusions could be drawn from the XRDP data.

Experimental Section

General: ^{1}H and ^{13}C NMR spectra were recorded with Bruker Avance DPX 400 or DRX 500 spectrometers; Scheme 2 shows the numbering scheme adopted for the ligands. Chemical shifts for ^{1}H and ^{13}C NMR spectra are referenced to residual solvent peaks with respect to TMS (δ = 0 ppm); all spectra were recorded at room temperature. FAB (NOBA matrix) mass spectra were recorded using a Finnigan MAT 8400 mass spectrometers. Ligands were prepared as previously reported.[7] AgBF$_4$ was used as received (Acros).

Silver(I) Complexes. General Method: All the complexes were prepared using the same procedure. One equivalent of AgBF$_4$ was combined with one equivalent of the ligand in MeCN (15 cm^3). The reaction mixture was sonicated for 5 min and then stirred under reflux for a further 15 min. The solvent was evaporated to give the crude silver(I) complex.

[Ag(4)$_2$][BF$_4$]: The reaction was carried out using ligand **4** (60 mg, 0.16 mmol) and AgBF$_4$ (31 mg, 0.16 mmol). [Ag(**4**)$_2$][BF$_4$] was isolated as a yellow solid (crude 77 mg). A small amount of analytically pure material was obtained by washing the crude material with water to remove excess AgBF$_4$. ^{1}H NMR (500 MHz, [D$_6$]-DMSO): δ = 8.80 (m, 2 H, H^{6A}), 8.76 (m, 2 H, H^{6C}), 8.56 (s, 2 H, H^{5B}), 8.55 (d, *J* = 8.0 Hz, 2 H, H^{3A}), 8.13 (td, *J* = 7.6, 2.0 Hz, 2 H, H^{4A}), 8.07 (td, *J* = 7.6, 1.6 Hz, 2 H, H^{4C}), 7.96 (d, *J* = 7.6 Hz, 2 H, H^{3C}), 7.67 (dd, *J* = 7.6, 5.2 Hz, 2 H, H^{5A}), 7.61 (dd, *J* = 7.6, 1.6 Hz, 2 H, H^{5C}), 2.82 [t, *J* = 6.0 Hz, 4 H, H$^{\mathrm{(ringB)C}H_2}$], 1.40 [m, 4 H, H$^{\mathrm{(ringB)CH_2C}H_2}$], 1.13 (m, 28 H, H$^{\mathrm{C}H_2}$), 0.79 (t, *J* = 6.8 Hz, 6 H, H$^{\mathrm{Me}}$) ppm. ^{13}C NMR (125 MHz, [D$_6$]DMSO): δ = 159.5, 155.6, 154.6, 151.1, 150.4, 149.4, 143.2, 138.5, 137.7, 126.5, 125.9, 124.8, 124.5, 122.4, 31.3 (C$^{\mathrm{ring}CH_2}$), 31.2 (C$^{\mathrm{alkyl}}$), 28.9 (C$^{\mathrm{alkyl}}$), 28.8 (C$^{\mathrm{alkyl}}$), 28.7 (C$^{\mathrm{alkyl}}$), 28.6 (C$^{\mathrm{alkyl}}$), 28.5 (C$^{\mathrm{alkyl}}$), 28.4 (C$^{\mathrm{alkyl}}$), 22.1 (C$^{\mathrm{alkyl}}$), 13.9 (C$^{\mathrm{Me}}$) ppm. FAB MS: *m*/*z* (%) = 375 [**4**]$^+$, 481 [Ag(**4**)]$^+$, 857 [Ag(**4**)$_2$]$^+$, 1052 [Ag$_2$(**4**)$_2$BF$_4$]$^+$. $C_{48}H_{60}AgBF_4N_8$ (943.72): calcd. C 61.09, H 6.41, N 11.87; found C 60.68, H 6.31, N 11.88.

[Ag(5)][BF$_4$]: The reaction was carried out with ligand **5** (80 mg, 0.24 mmol) and AgBF$_4$ (46 mg, 0.24 mmol). [Ag(**5**)][BF$_4$] was isolated as a yellow solid (120 mg, 0.23 mmol, 93%). ^{1}H NMR (500 MHz, [D$_6$]DMSO): δ = 8.91 (d, *J* = 4.0 Hz, 1 H, H^{6A}), 8.77 (m, 2 H, H^{5B+6C}), 8.60 (d, *J* = 8.0 Hz, 1 H, H^{3A}), 8.19 (td, *J* = 8.0, 2.0 Hz, 1 H, H^{4A}), 7.88 (m, 3 H, H^{4C+3D}), 7.79 (dd, *J* = 7.6, 5.2 Hz, 1 H, H^{5A}), 7.60 (dd, *J* = 7.6, 5.2 Hz, 1 H, H^{5C}), 7.44 (d, *J* = 8.0 Hz, 3 H, H^{2D+3C}) ppm. ^{13}C NMR (125 MHz, [D$_6$]DMSO): δ = 157.4, 155.3, 152.1, 150.8, 150.6, 149.6, 139.9, 139.8, 138.9, 137.7, 132.5, 130.1, 127.8, 126.7, 126.2, 125.3, 123.7, 118.2, 111.9 ppm. FAB-MS: *m*/*z* (%) = 442 [Ag(**5**)]$^+$, 778 [Ag(**5**)$_2$]$^+$, 973 [Ag$_2$(**5**)$_2$BF$_4$]$^+$. $C_{21}H_{13}AgBF_4N_5\cdot{}^2/_3MeCN$ (557.37): calcd. C 48.09, H 2.71, N 14.25; found C 49.03, H 2.81, N 13.79.

[Ag(6)][BF$_4$]: The reaction was carried out with ligand **6** (70 mg, 0.20 mmol) and AgBF$_4$ (38 mg, 0.19 mmol). [Ag(**6**)][BF$_4$] was isolated as a yellow solid (93 mg, 0.17 mmol, 85%). ^{1}H NMR (500 MHz, [D$_6$]DMSO): δ = 8.83 (ddd, *J* = 4.8, 1.6, 0.8 Hz, 1 H, H^{6A}), 8.69 (d, *J* = 7.9 Hz, 1 H, H^{3A}), 8.63 (s, 1 H, H^{5B}), 8.39 (ddd, *J* = 4.8, 1.6, 0.9 Hz, 1 H, H^{6C}), 8.22 (d, *J* = 8.9 Hz, 2 H, H^{2D}), 8.13 (td, *J* = 7.8, 1.8 Hz, 1 H, H^{4A}), 8.08 (d, *J* = 7.7 Hz, 1 H, H^{3C}), 8.03 (td, *J* = 7.7, 1.7 Hz, 1 H, H^{4C}), 7.65 (ddd, *J* = 7.6, 4.8, 1.1 Hz, 1 H, H^{5A}), 7.60 (d, 2 H, H^{3D}), 7.46 (ddd, *J* = 7.4, 4.8, 1.3 Hz, 1 H, H^{5C}) ppm. ^{13}C NMR (125 MHz, [D$_6$]DMSO): δ = 157.5, 155.6, 152.4, 150.7, 150.3, 150.0, 147.6, 142.2, 139.3, 138.8, 137.7, 130.6, 127.5, 126.6, 125.1, 123.6, 123.3 ppm. FAB-MS: *m*/*z* = 462 [Ag(**6**)]$^+$, 817 [Ag(**6**)$_2$]$^+$, 1013 [Ag$_2$(**6**)$_2$BF$_4$]$^+$. $C_{20}H_{13}AgBF_4N_5O_2$ (550.02): calcd. C 43.67, H 2.38, N 12.73; found C 43.82, H 2.80, N 12.70.

[Ag(7)][BF$_4$]: The reaction was carried out with ligand **7** (55 mg, 0.16 mmol) and AgBF$_4$ (32 mg, 0.16 mmol). [Ag(**7**)][BF$_4$] was isolated as a white solid (68 mg, 0.13 mmol, 82%). ^{1}H NMR (400 MHz, [D$_6$]DMSO): δ = 8.91 (d, *J* = 4.1 Hz, 1 H, H^{6A}), 8.84 (d, *J* = 4.6 Hz, 1 H, H^{6C}), 8.64 (s, 1 H, H^{5B}), 8.59 (d, *J* = 8.1 Hz, 1 H, H^{3A}), 8.16 (td, *J* = 7.9, 1.7 Hz, 1 H, H^{4A}), 7.85 (td, *J* = 7.8, 1.6 Hz, 1 H, H^{4C}), 7.78 (dd, *J* = 6.8, 4.8 Hz, 1 H, H^{5A}), 7.61 (dd, *J* = 8.0, 4.8 Hz, 1 H, H^{5C}), 7.33 (d, *J* = 7.9 Hz, 1 H, H^{3C}), 7.15 (d, *J* = 8.8 Hz, 2 H, H^{3D}), 6.95 (d, *J* = 8.9 Hz, 2 H, H^{2D}), 3.78 (s, 3 H, H$^{\mathrm{Me}}$) ppm. ^{13}C NMR (100 MHz, [D$_6$]DMSO): δ = 160.4, 157.7, 155.1, 153.0, 150.8, 150.7, 150.0, 141.0, 138.9, 137.6, 130.8 (C^{2D}), 127.2, 126.8, 126.6, 126.2, 125.2, 123.6, 114.3 (C^{3D}), 55.4 (C$^{\mathrm{Me}}$) ppm. FAB MS: *m*/*z* = 448 [Ag(**7**)]$^+$, 787 [Ag(**7**)$_2$]$^+$, 983 [Ag$_2$(**7**)$_2$BF$_4$]$^+$. $C_{21}H_{16}AgBF_4N_4O$ (535.05): calcd. C 47.14, H 3.01, N 10.47; found C 47.72, H 3.25, N 10.72.

[Ag(8)][BF$_4$]: The reaction was carried out using ligand **8** (40 mg, 0.11 mmol) and AgBF$_4$ (20 mg, 0.10 mmol). [Ag(**8**)][BF$_4$] was isolated as a pale red solid (46 mg, 0.080 mmol, 73%). ^{1}H NMR (400 MHz, CD$_3$CN): δ = 8.83 (d, *J* = 4.3 Hz, 1 H, H^{6A}), 8.70 (d, *J* = 4.6 Hz, 1 H, H^{6C}), 8.44 (s, 1 H, H^{5B}), 8.35 (d, *J* = 8.0 Hz, 1 H, H^{3A}), 8.07 (td, *J* = 7.9, 1.5 Hz, 1 H, H^{4A}), 7.73 (td, *J* = 7.8, 1.6 Hz, 1 H, H^{4C}), 7.68 (m, 3 H, H^{3D+5A}), 7.62 (dd, *J* = 7.6, 5.2 Hz, 1 H, H^{5C}), 7.36 (d, *J* = 8.0 Hz, 2 H, H^{2D}), 7.33 (d, *J* = 7.8 Hz, 1 H, H^{3C}) ppm. ^{13}C NMR (100 MHz, CD$_3$CN): δ = /ppm: 158.9 (C$^{3B/6B}$), 157.0 (C$^{3B/6B}$), 153.7 (C^{2C}), 151.9 (C^{6A}), 151.8 (C^{6C}), 151.4 (C^{2A}), 141.5 (C$^{1D/4B}$), 140.6 (C$^{1D/4B}$), 139.9 (C^{4A}), 138.7 (C^{4C}), 131.6 (q, J_{CF} = 38 Hz, C^{4D}), 131.0 (C^{2D}), 128.8 (C^{5B}), 127.6 (C$^{3C/5A}$), 127.5 (C$^{3C/5A}$), 126.8 (q, J_{CF} = 3.8 Hz, C^{3D}), 126.2 (C^{5C}), 125.1 (q, J_{CF} = 265 Hz, C$^{\mathrm{CF_3}}$), 124.4 (C^{3A}). FAB MS: *m*/*z* = 486 [Ag(**8**)]$^+$, 864 [Ag(**8**)$_2$]$^+$, 1059 [Ag$_2$(**8**)$_2$BF$_4$]$^+$. $C_{21}H_{13}AgBF_7N_4$ (573.02): calcd. C 44.02, H 2.29, N 9.78; found C 43.36, H 2.53, N 9.45.

[Ag(9)][BF$_4$]: The reaction was carried out using ligand **9** (60 mg, 0.13 mmol) and AgBF$_4$ (25 mg, 0.13 mmol). [Ag(**9**)][BF$_4$] was isolated as a yellow solid (46 mg, 0.069 mmol, 53%). ^{1}H NMR (400 MHz, [D$_6$]DMSO): δ = 8.91 (d, *J* = 4.0 Hz, 1 H, H^{6A}), 8.79 (s, 1 H, H^{5B}), 8.74 (d, *J* = 4.4 Hz, 1 H, H^{6C}), 8.63 (d, *J* = 8.0 Hz, 1 H, H^{3A}), 8.20 (td, *J* = 8.0, 1.6 Hz, 1 H, H^{4A}), 7.96 (m, 2 H, H^{4C+4D}), 7.79 (dd, *J* = 7.6, 5.2 Hz, 1 H, H^{5A}), 7.60 (m, 2 H, H^{5C+3C}), 7.49 (d, *J* = 1.6 Hz, 2 H, H^{2D}) ppm. ^{13}C NMR (100 MHz, [D$_6$]DMSO): δ = 157.5, 155.3, 152.3, 150.8, 150.4, 149.7, 139.0, 138.9, 138.3, 137.7, 133.9, 130.9, 127.7, 126.6, 126.1, 125.1, 123.6, 122.4 ppm. FAB MS: *m*/*z* = 575 [Ag(**9**)]$^+$, 1043 [Ag(**9**)$_2$]$^+$, 1239 [Ag$_2$(**9**)$_2$BF$_4$]$^+$. $C_{20}H_{12}AgBBr_2F_4N_4\cdot{}^1/_2H_2O$ (671.82): calcd. C 35.76, H 1.95, N 8.34; found C 35.69, H 2.14, N 8.33.

[Ag(10)$_2$][BF$_4$]: The reaction was carried out using ligand **10** (60 mg, 0.16 mmol) and AgBF$_4$ (32 mg, 0.16 mmol). [Ag(**10**)$_2$][BF$_4$] was isolated as a yellow solid (crude 69 mg). Attempts were made to purify the bulk sample by washing with water, but analytically pure material could not be obtained. ^{1}H NMR (500 MHz, [D$_6$]-DMSO): δ = 8.90 (d, *J* = 4.1 Hz, 2 H, H^{6A}), 8.83 (d, *J* = 4.6 Hz, 2

H, H^{6C}), 8.73 (s, 2 H, H^{5B}), 8.62 (d, J = 8.1 Hz, 2 H, H^{3A}), 8.18 (td, J = 7.8, 1.7 Hz, 2 H, H^{4A}), 7.89 (td, J = 7.8, 1.6 Hz, 2 H, H^{4C}), 7.78 (ddd, J = 7.6, 5.1, 1.0 Hz, 2 H, H^{5A}), 7.62 (dd, J = 7.6, 5.2 Hz, 2 H, H^{5C}), 7.41 (d, J = 7.9 Hz, 2 H, H^{3C}), 6.58 (t, J = 2.2 Hz, 2 H, H^{4D}), 6.40 (d, J = 2.2 Hz, 4 H, H^{2D}), 3.65 (s, 6 H, H^{Me}) ppm. ^{13}C NMR (125 MHz, [D$_6$]DMSO): δ = 150.5, 150.4, 138.7, 137.6, 137.3, 127.3, 125.9, 124.9, 123.5, 107.1, 100.8, 55.4 (C^{Me}), quat ppm. C not observed. FAB MS: m/z = 477 $[Ag(\mathbf{10})]^+$, 847 $[Ag(\mathbf{10})_2]^+$, 1043 $[Ag_2(\mathbf{10})_2BF_4]^+$.

Crystal Structure Determinations: General: Data were collected on an Enraf Nonius Kappa CCD instrument; data reduction, solution and refinement used the progams COLLECT,[19] SIR92,[20] DENZO/SCALEPACK[21] and CRYSTALS.[22] Structures have been analyzed using Mercury v. 1.4.2.[23]

Crystal Data for $[Ag(\mathbf{4})_2][BF_4]$: $C_{48}H_{60}AgBF_4N_8$, M = 943.73, triclinic, space group $P\bar{1}$, a = 8.1443(7), b = 24.585(2), c = 25.804(2) Å, α = 115.007(4), β = 98.246(4), γ = 97.300(4)°, U = 4531.2(6) Å^3, Z = 4, D_c = 1.383 Mg m^{-3}, μ(Mo-K_α) = 0.505 mm^{-1}, T = 173 K, 14192 reflections collected. Refinement of 10252 reflections (1117 parameters) with $I > 2.0\sigma(I)$ converged at final R_1 = 0.0653 (R_1 all data = 0.1176), wR_2 = 0.1592 (wR_2 all dat$a$ = 0.2018), gof = 0.977.

Crystal Data for $[Ag_2(\mathbf{5})_2][BF_4]_2$: $C_{42}H_{26}Ag_2B_2F_8N_{10}$, M = 1060.08, monoclinic, space group $P2_1/c$, a = 10.0117(9), b = 9.835(1), c = 19.485(1) Å, β = 95.780(6)°, U = 1908.9(3) Å^3, Z = 2, D_c = 1.844 Mg m^{-3}, μ(Mo-K_α) = 1.115 mm^{-1}, T = 173 K, 4383 reflections collected. Refinement of 3148 reflections (289 parameters) with $I > 3.0\sigma(I)$ converged at final R_1 = 0.0359 (R_1 all data = 0.0412), wR_2 = 0.0305 (wR_2 all data = 0.0315), gof = 1.047.

Crystal Data for $\{[Ag_2(\mathbf{6})_2(NCMe)_2][BF_4]_2\cdot Et_2O\}_n$: $C_{48}H_{42}Ag_2B_2F_8N_{12}O_5$, M = 1256.28, monoclinic, space group $P2_1/c$, a = 14.2235(5), b = 12.1001(5), c = 29.266(1) Å, β = 94.027(2)°, U = 5024.5(3) Å^3, Z = 4, D_c = 1.661 Mg m^{-3}, μ(Mo-K_α) = 0.869 mm^{-1}, T = 173 K, 8400 reflections collected. Refinement of 8323 reflections (721 parameters) with $I > 2.0\sigma(I)$ converged at final R_1 = 0.0578 (R_1 all data = 0.1144), wR_2 = 0.1385 (wR_2 all data = 0.1818), gof = 1.001.

Crystal Data for $\{[Ag_3(\mathbf{7})_2][BF_4]_3\}_n$: $C_{42}H_{30}Ag_3B_3F_{12}N_8O_2$, M = 1264.78, monoclinic, space group $C2/c$, a = 25.5134(2), b = 11.6105(1), c = 17.6852(2) Å, β = 122.0663(4)°, U = 4439.51(7) Å^3, Z = 4, D_c = 1.892 Mg m^{-3}, μ(Mo-K_α) = 1.409 mm^{-1}, T = 173 K, 6493 reflections collected. Refinement of 4328 reflections (344 parameters) with $I > 3.0\sigma(I)$ converged at final R_1 = 0.0266 (R_1 all data = 0.0438), wR_2 = 0.0239 (wR_2 all data = 0.0415), gof = 1.258.

Crystal Data for $[Ag_2(\mathbf{8})_2][BF_4]_2\cdot 2.6MeCN$: $C_{47.2}H_{33.8}Ag_2B_2F_{14}N_{10.6}$, M = 1252.79, monoclinic, space group $C2/c$, a = 12.7058(5), b = 10.9051(4), c = 35.415(1) Å, β = 93.137(1)°, U = 4899.6(3) Å^3, Z = 4, D_c = 1.698 Mg m^{-3}, μ(Mo-K_α) = 0.900 mm^{-1}, T = 173 K, 5587 reflections collected. Refinement of 4350 reflections (415 parameters) with $I > 3.0\sigma(I)$ converged at final R_1 = 0.0326 (R_1 all data = 0.0448), wR_2 = 0.0339 (wR_2 all data = 0.0371), gof = 1.128.

Crystal Data for $[Ag_2(\mathbf{9})_2][BF_4]_2\cdot 2MeCN$: $C_{44}H_{30}Ag_2B_2Br_4F_8N_{10}$, M = 1407.75, monoclinic, space group $P2_1/a$, a = 8.1005(9), b = 34.509(4), c = 8.4695(8) Å, β = 97.13(1)°, U = 2349.3(4) Å^3, Z = 4, D_c = 1.990 Mg m^{-3}, μ(Mo-K_α) = 4.313 mm^{-1}, T = 173 K, 6410 reflections collected. Refinement of 4025 reflections (316 parameters) with $I > 3.0\sigma(I)$ converged at final R_1 = 0.0405 (R_1 all data = 0.0720), wR_2 = 0.0455 (wR_2 all data = 0.0700), gof = 1.040.

Crystal Data for $[Ag(\mathbf{10})_2][BF_4]$: $C_{44}H_{36}AgBF_4N_8O_4$, M = 935.49, monoclinic, space group $C2/c$, a = 34.923(2), b = 6.6039(8), c = 20.747(1) Å, β = 123.92(1)°, U = 3970.4(8) Å^3, Z = 4, D_c = 1.565 Mg m^{-3}, μ(Mo-K_α) = 0.583 mm^{-1}, T = 173 K, 4209 reflections collected. Refinement of 3113 reflections (300 parameters) with $I > 2.0\sigma(I)$ converged at final R_1 = 0.0380 (R_1 all data = 0.0572), wR_2 = 0.0410 (wR_2 all data = 0.0437), gof = 1.194.

CCDC-678489 (for $[Ag(\mathbf{4})_2][BF_4]$), -678490 (for $[Ag_2(\mathbf{5})_2][BF_4]_2$), -678487 (for $\{[Ag_2(\mathbf{6})_2(NCMe)_2][BF_4]_2\cdot Et_2O\}_n$), -678491 (for $\{[Ag_3(\mathbf{7})_2][BF_4]_3\}_n$), -678485 (for $[Ag_2(\mathbf{8})_2][BF_4]_2\cdot 2.6MeCN$), -678486 (for $[Ag_2(\mathbf{9})_2][BF_4]_2\cdot 2MeCN$) and -678488 (for $[Ag(\mathbf{10})_2][BF_4]$) contain the supplementary crystallographic data. These data can be obtained free of charge from The Cambridge Crystallographic Data Centre via www.ccdc.cam.ac.uk/data_request/cif.)

Acknowledgments

The Swiss National Science Foundation and the University of Basel are acknowledged for financial support. We would like to thank Katharina Fromm and Laurent Mirolo (University of Fribourg) for carrying out the powder X-ray data collections.

---

[1] Z. Xu, L. K. Thompson in *Comprehensive Coordination Chemistry II* (Eds.: J. A. McCleverty, T. J. Meyer), Elsevier, Oxford, **2004**, vol. 1, pp. 63–95.

[2] M.-T. Youinou, N. Rahmouni, J. Fischer, J. A. Osborn, *Angew. Chem. Int. Ed. Engl.* **1992**, *31*, 733–735.

[3] B. L. Schottel, H. T. Chifotides, M. Shatruk, A. Chouai, L. M. Pérez, J. Bacsa, K. R. Dunbar, *J. Am. Chem. Soc.* **2006**, *128*, 5895–5912.

[4] E. C. Constable, C. E. Housecroft, B. M. Kariuki, M. Neuburger, C. B. Smith, *Aust. J. Chem.* **2003**, *56*, 653–655.

[5] E. C. Constable, C. E. Housecroft, M. Neuburger, S. Reymann, S. Schaffner, *Chem. Commun.* **2004**, 1056–1057.

[6] A. G. Young, L. R. Hanton, *Coord. Chem. Rev.* **2007**, DOI:10.1016/j.ccr. 2007.07.017.

[7] E. C. Constable, C. E. Housecroft, M. Neuburger, S. Reymann, S. Schaffner, *Eur. J. Org. Chem.* **2008**, in press.

[8] E. C. Constable, C. E. Housecroft, B. M. Kariuki, N. Kelly, C. B. Smith, *Inorg. Chem. Commun.* **2002**, *5*, 199–202.

[9] E. C. Constable, C. E. Housecroft, M. Neuburger, S. Reymann, S. Schaffner, *CrystEngComm*, **2008**, submitted.

[10] S. Ghumaan, B. Sarker, S. Patra, K. Parimal, J. van Slageren, J. Fiedler, W. Kaim, G. K. Lahiri, *Dalton Trans.* **2005**, 706–712.

[11] R. Hoogenboom, G. Kickelbick, U. S. Schubert, *Eur. J. Org. Chem.* **2003**, *24*, 4887–4896.

[12] R. A. Russell, D. E. Marsden, M. Sterns, R. N. Warrener, *Aust. J. Chem.* **1981**, *34*, 1223–1234.

[13] M. Balogh, P. Laszlo, K. Simon, *J. Org. Chem.* **1987**, *52*, 2026–2029.

[14] M. J. Haddadin, Y. Wang, S. Frenkel, S. G. Bott, L. Yang, P. S. Braterman, C. Carvallo, A. P. Marchand, W. H. Watson, R. P. Kashyap, M. Krawiec, S. A. Borne, *Heterocycles* **1994**, *37*, 869–882.

[15] W. H. Watson, R. P. Kashyap, M. Krawiec, D. Sun, T. F. Carlson, A. P. Marchand, Y. Wang, *J. Chem. Crystallogr.* **1994**, *24*, 259–266.

[16] M. Mascal, J.-L. Kerdelhué, A. J. Blake, P. A. Cooke, *Angew. Chem. Int. Ed.* **1999**, *38*, 1968–1971.

[17] See for example: M. Munakata, L. P. Wu, T. Kuroda-Sowa, M. Maekawa, Y. Suenaga, G. L. Ning, T. Kojima, *J. Am. Chem. Soc.* **1998**, *120*, 8610–8618.

[18] E. C. Constable, C. E. Housecroft, B. M. Kariuki, N. Kelly, C. B. Smith, *C. R. Chim.* **2002**, *5*, 425–430.

[19] *COLLECT Software*, Nonius BV **1997**–2001.

[20] A. Altomare, G. Cascarano, G. Giacovazzo, A. Guagliardi, M. C. Burla, G. Polidori, M. Camalli, *J. Appl. Crystallogr.* **1994**, *27*, 435–435.

[21] Z. Otwinowski, W. Minor, *Methods in Enzymology*, vol. 276 (Eds.: C. W. Carter, R. M. Sweet Jr), **1997**, Academic Press, New York, p. 307.

[22] P. W. Betteridge, J. R. Carruthers, R. I. Cooper, K. Prout, D. J. Watkin, *J. Appl. Crystallogr.* **2003**, *36*, 1487–1487.

[23] I. J. Bruno, J. C. Cole, P. R. Edgington, M. K. Kessler, C. F. Macrae, P. McCabe, J. Pearson, R. Taylor, *Acta Crystallogr., Sect. B* **2002**, *58*, 389–397.

Received: March 19, 2008